Journal of Macromolecular Science, Part A
Publication details, including instructions for authors and subscription information:
http://www.informaworld.com/smpp/title~content=t713597274

TRANSPARENT, ABRASION-RESISTANT COATINGS FOR METAL SUBSTRATES

Kurt Jordens[a]; Garth Wilkes[b]
[a] Texas Eastman Division, Eastman Chemical Company, Longview, TX, U.S.A. [b] Department of Chemical Engineering, Polymer Materials and Interfaces Laboratory, The Center for Adhesive and Sealant Science, Virginia Tech, Blacksburg, VA, U.S.A.

Online publication date: 14 February 2001

To cite this Article Jordens, Kurt and Wilkes, Garth(2001) 'TRANSPARENT, ABRASION-RESISTANT COATINGS FOR METAL SUBSTRATES', Journal of Macromolecular Science, Part A, 38: 2, 185 — 207
To link to this Article: DOI: 10.1081/MA-100103342
URL: http://dx.doi.org/10.1081/MA-100103342

J. MACROMOL. SCI.—PURE APPL. CHEM., A38(2), 185–207 (2001)

TRANSPARENT, ABRASION-RESISTANT COATINGS FOR METAL SUBSTRATES

Kurt Jordens† and Garth Wilkes*

Department of Chemical Engineering, Polymer Materials and Interfaces Laboratory, The Center for Adhesive and Sealant Science, Virginia Tech, Blacksburg, VA 24061-0211

ABSTRACT

Novel hybrid inorganic-organic network materials have been synthesized and applied as transparent abrasion-resistant coatings for metal substrates. A specially functionalized low molecular weight organic material (diethylenetriamine) served as a precursor for all coating formulations. Combination of this functionalized organic material with metal alkoxide(s) and other alkoxysilane functional materials in the sol–gel reaction led to hybrid inorganic–organic chemical networks. While still a liquid, the initiated coating formulations were applied to the desired metal substrates by a spin coating process followed by thermal curing. The substrates used in this study included aluminum, plain steel, conversion coated steel, stainless steel, copper, and brass. A fluorinated monomer has also been utilized in selected cases to tailor the surface-free energy of the coatings. Such coatings displayed a linear increase in the water contact angle with increasing mass fraction of fluorinated monomer in the formulation. Other formulations have been explored that contain an ultraviolet absorbing species. The effects of coating formulation, cure temperature, and cure time on abrasion resistance have been determined.

Key Words: Ceramer; Coating; Abrasion; Sol-gel; Fluorinated; Ultraviolet absorber.

*Corresponding author.
†Current address: Texas Eastman Division, Eastman Chemical Company, P.O. Box 7444, Longview, TX 75607-7444.

INTRODUCTION

In 1985, the term *ceramer* was coined, which combined the words *cera*mic and poly*mer* or oligo*mer* (1). The first such material was generated by the sol–gel reaction of hydroxyl terminated poly(dimethylsiloxane) oligomers and tetraethoxysilane. The result was a novel hybrid network material. More recently, research in the ceramer area has evolved into the preparation of transparent, abrasion-resistant coatings. These coatings were first applied to bisphenol–A polycarbonate substrates (PC), which put an upper constraint on the cure temperature of the coatings, set by the glass transition temperature of PC (≈145°C). Some of the varied organic components in these coatings were *bis* and *tris* maleimides (2), melamine and *tris*(m–aminophenyl) phosphine oxide (3), 4,4'–diaminodiphenylsulfone (4), diethylenetriamine (4–6) several aliphatic diols, resorcinol, iminobispropylamine, and poly(ethyleneimine) (5,6). Some coating formulations have been altered to include an ultraviolet (UV) absorbing species to protect the PC substrate and enhance the lifetime of the coatings (7). The present report focuses on similar coatings based on alkoxysilane functionalized diethylenetriamine, however, applied to metal substrates. This allowed the exploration of higher cure temperatures (i.e., not limited by the substrate as was the case for PC). Also, new formulations included a fluorinated species, which systematically lowered the surface-free energy of the final coatings. The coatings addressed in this work can be used in many applications where an abrasion-resistant coating is desired for a metal surface. Some possibilities include vehicles, military applications, metallic receptacles, and décor.

EXPERIMENTAL

Materials

Diethylenetriamine (DETA) 99% pure, ethylacetoacetate (EAcAc) 99+%, aluminum tri-*sec*-butoxide (Al) 97%, 3–(aminopropyl)triethoxysilane 99%, 3–(trimethoxysilyl)-propyl methacrylate 97% (MASi), and 1N HCl, were purchased from Aldrich and used as received. Tetramethoxysilane (TMOS) 99+% pure, isocyanatopropyltriethoxysilane (ICPTES) 95%, and 3,3,3–(trifluoropropyl) trimethoxysilane were obtained from United Chemical Technologies, Inc., PETRARCH® silanes and silicones, and Gelest, Inc., and used as purchased. 2–Propanol (IPA) and acetone, ACS specifications, were used as received from Mallinckrodt Analytical Reagents. Norbloc 7966, a UV absorbing molecule, was obtained from Noramco Inc. of New Brunswick, NJ.

The substrates chosen for study include: aluminum (0.020″ thick, complies with ASTM D1730), plain steel (0.020″, complies with ASTM D609 type 3 A366), and both zinc phosphate and iron phosphate conversion coated steels (0.020″), purchased from Q Panel; also stainless steel (0.036″, type 304, 2B fin-

ish), copper (0.032″, complies to federal specification QQ-C-576, ASTM B152, type ETP), and brass (0.032″, QQ-B-613, alloy 260, ASTM B19, B36) purchased from McMaster Carr; and finally a chemically cleaned, highly polished aluminum alloy (5657-H18). All panels were cut to a size between ≈ 3″× 3″ and 4″× 4″, which were then used as the substrates.

The aluminum, steel, and copper substrates were first sanded with emery paper using an electric hand–held sander and washed with either acetone or IPA before application of the coating formulations. The surface characteristics of the sanded aluminum and sanded steel are shown in the scanning electron microscopy images of Figures 1 and 2, respectively. The aluminum surface is well roughened by the sanding process. The steel displays a smoother surface with curved scratches, which are generated by the circular motion of the sander. The varied response for the two substrates is likely dominated by the difference in hardness of the two metals. The harder steel is less affected by the action of the aluminum oxide particles from the emery paper.

Because the conversion coated steels, stainless steel, brass, and polished aluminum alloy substrates contained polished, cosmetic surfaces, they were only washed with either IPA or acetone before coating application.

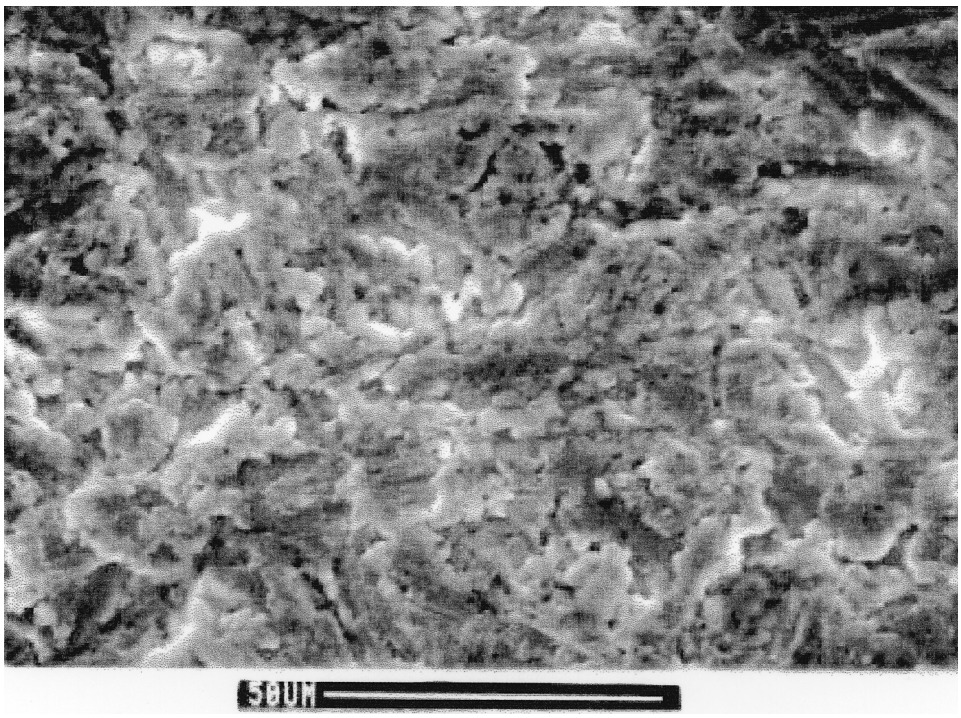

Figure 1. SEM image of emery sanded aluminum substrate. 50-μm marker.

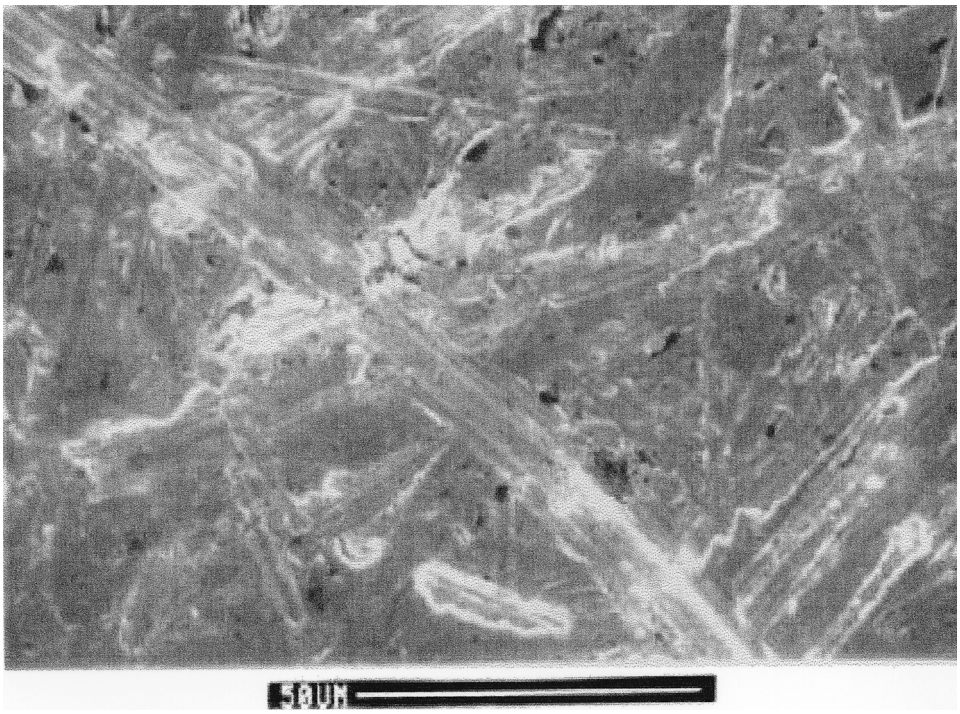

Figure 2. SEM image of emery sanded, plain steel substrate. 50-μm marker.

Instrumentation

A Cambridge Stereoscan 200 scanning electron microscope (SEM) was used at 15 to 20 kV to examine surface features at high magnifications. All SEM samples were first sputter–coated with gold in a Bal–Tec SCD005 sputter coater in an argon plasma.

Fourier transform Infrared spectroscopy (FT-IR) was performed on a Nicolet instrument.

A Taber Abraser standardized abrasion test apparatus was used with 500 g of load on Calibrase CS-10 wheels. These wheels are composed of aluminum oxide particles embedded in a rubber matrix and were refreshed every 350–500 cycles with the abrasive disks described by the manufacturer. The primary abrasive particle size is ~10 μm, and agglomerations of particles are ~100 μm, as observed by SEM. During the abrasion tests, a steady flow of dry air was passed over the coated samples to remove wear debris from the sample surface. The number of cycles employed in the abrasion tests was varied, depending on the substrate type.

Water contact angles were measured at room temperature with a contact angle goniometer using deionized water. At least eight measurements were made per sample, and a statistical average was derived from these eight measurements.

An attempt at quantification of the strength of the adhesive bond between the coating and the substrate has been undertaken with a direct pull off test (8). In this experiment, an Instron (model 4204) was utilized in tension in an effort to remove the coating from the substrate using a specially designed apparatus, illustrated in Figure 3. If failure from this test occurred between the coating and substrate, then dividing this failure load by the cross–sectional area of the failure surface yields a practical strength of adhesion.

All coated samples that are shown as images are *not* photographs (unless noted), but rather scans of actual samples. This was accomplished with a flat–bed, Hewlett Packard ScanJet 4P. A piece of transparent overhead film was laid between the coated samples and the scanner to prevent the samples from scratching the surface of the scanner glass. Images were modified electronically to maximize the visibility of wear tracks and other important features.

Coating Preparation

Triethoxysilane Functionalization of Diethylenetriamine

The first step in the coating preparation involved the synthesis of triethoxysilane functionalized DETA, a monomer that is later used in the coating formulations. This was achieved by mixing 5.00 g of DETA with 18.37 g IPA in a round-bottom flask, which was immediately submerged in an ice bath (to prevent unwanted side reactions). In a separatory funnel was placed 39.76 g of ICPTES (this corresponds to a slight excess of ICPTES, or 3.05 moles per mole DETA) and this liquid was added dropwise to the DETA-IPA mixture over the course of ≈30 min. A DETA molecule ideally combines with three ICPTES molecules form-

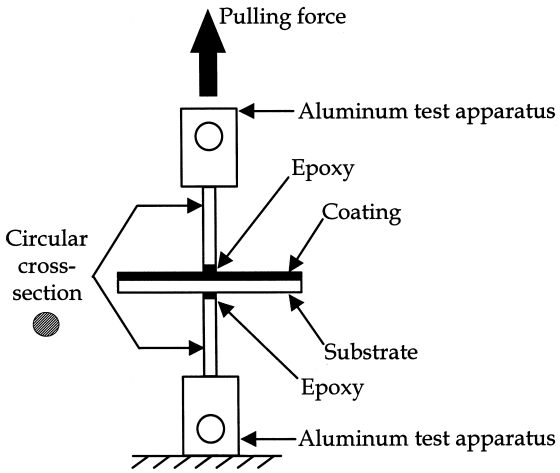

Figure 3. A schematic of the direct pull off testing apparatus used to ascertain a practical value of adhesion between coatings and substrates.

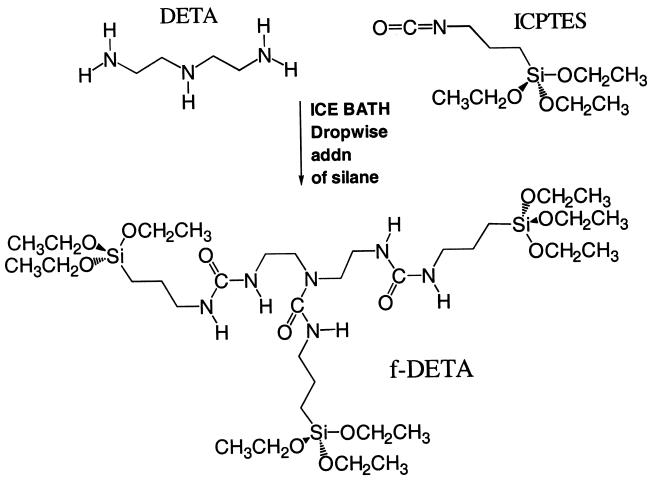

Figure 4. Functionalization of diethylenetriamine (DETA) with isocyanato-propyltriethoxysilane (ICPTES) to form the coating precursor, functionalized DETA (f-DETA).

ing three urea linkages, as illustrated in Figure 4. When the addition of ICPTES was complete (30 min), the roundbottom flask was sealed with septa and the mixture was stirred in the ice bath for 8 h. After this period the reaction was complete as determined by the disappearance of the isocyanate peak from FT-IR spectroscopy (≈2273 cm^{-1}). The product of this reaction will be referred to as f-DETA (alkoxysilane functionalized DETA solution) throughout the remainder of this manuscript. Note that the f–DETA species is present in a solution with IPA (70 wt% f-DETA), as a result of this synthetic approach.

f-DETA(100) Coating Formulation and Procedures

The second step in the coating preparation involved sol-gel chemistry. The f-DETA solution, either in the neat form or with added metal alkoxide(s) and other components, will undergo hydrolysis and polycondensation in the presence of water and either acid or base catalyst by the well known sol–gel reaction. Note that the water used in all coating formulations was derived from the aqueous acid catalyst and the moisture in the ambient air. A typical recipe for a coating based on f-DETA without additional metal alkoxide or other components [labeled f-DETA(100)] was made by combining 3.00 g of f-DETA solution with 1.50 g of IPA and stirring. This was followed by the dropwise addition of 0.15 g of aqueous 0.5 M HCl while under brisk stirring. This reaction is shown schematically in Figure 5. After stirring for ≈1 min, this liquid was applied by a spin coating process to the desired substrate. Note that the viscosity of this reacting solution will rapidly increase due to the build-up of molecular weight during the sol-gel reaction. Spin coating was accomplished with a simple turntable device with a variable transformer that controls the rotation rate (generally ≈3000 rpm). The

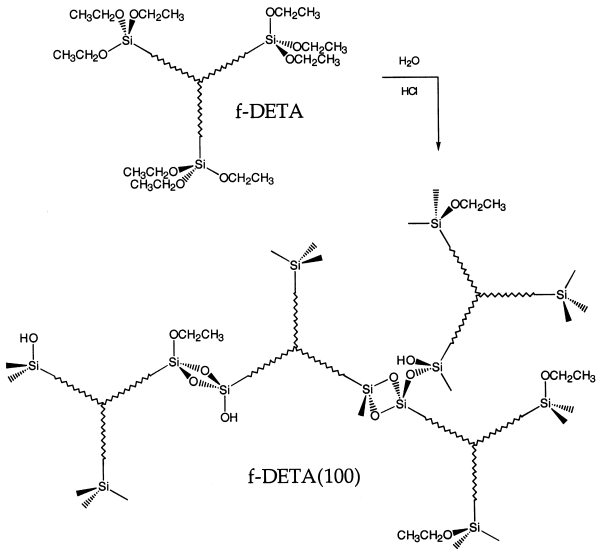

Figure 5. The sol–gel reaction of f-DETA (simplified representation), forming a coating designated as f-DETA(100). The structure is meant to reflect an infinite network.

substrates were attached to the turntable with double–stick tape, and the liquid coating was applied by pipette onto the center of the substrates (which may be already rotating or not). After the spin-coating process, the samples were set under cover (away from dust) until the coating reached a nontack state (≈5 to 10 min). After this, the coated samples were transferred to a forced–convection oven, where they were exposed to the desired temperature program. A typical cure schedule involved holding at 60°C for 30 min, heating to 175°C at a rate of 5°/min, and holding at this temperature for 1 h. Other temperatures and cure times were also explored to determine the effects of these variables on the resulting coating performance.

f-DETA(50) TMOS(50) Coating Formulation

A coating comprised of 50% f–DETA and 50% TMOS by weight [f-DETA(50) TMOS(50)] was generated by combining 2.00 g f-DETA solution, 1.00 g IPA, and 1.40 g TMOS under stirring. This was followed by the dropwise addition of 0.25 g of 0.5 M HCl under brisk stirring. This reaction is shown schematically in Figure 6. The coating was then applied and cured as before.

Fluorinated Coating Formulations

The surface-free energies of the ceramer coatings have also been tailored in selected cases. In an attempt to lower the surface free energy of some of the coatings (i.e., create a hydrophobic surface), a fluorinated monomer was added to the

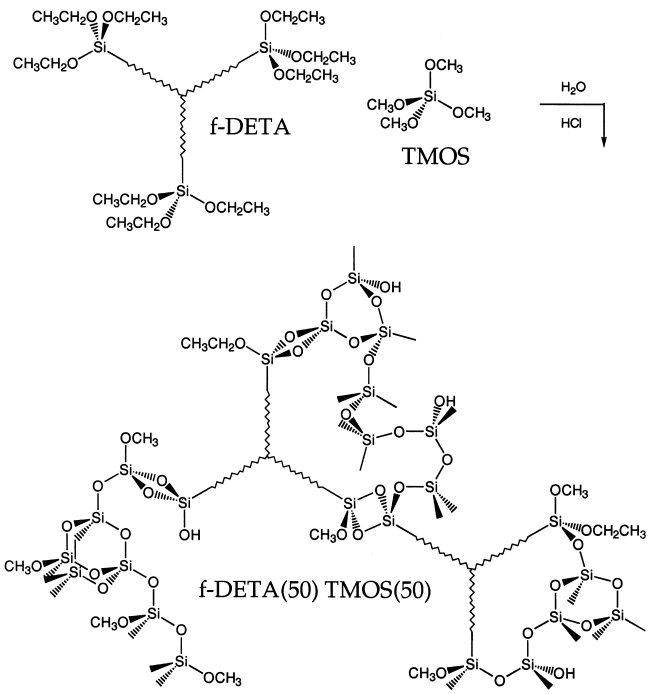

Figure 6. The sol–gel reaction of f-DETA with TMOS, forming a coating designated as f-DETA(50) TMOS(50). The resulting structure is meant to reflect an infinite network.

coating formulation (9). Namely, (3,3,3–trifluoropropyl)trimethoxysilane was introduced into the network oxide. The trimethoxysilane groups of this molecule can participate in the sol–gel reaction and, hence, the fluorinated species will be covalently bonded to the network. This is more desirable than simply adding a nonbonded fluorinated species to the coatings, which could diffuse out of the coating, leading to an undesirable change in the surface-free energy with time. Hence the covalently bonded, fluorinated molecules provide a more persistent value of surface-free energy of the resulting coatings. A typical fluorinated coating [denoted as f-DETA(47.5)-TMOS(47.5)-F(5)] was made by combining 2.00 g IPA, 4.00 g f-DETA, 2.80 g TMOS, and 0.295 g (3,3,3–trifluoropropyl) trimethoxysilane (F) and stirring. This was followed by the dropwise addition of 0.52 g 0.5 M HCl. The modified coating was then applied to the desired substrate and thermally cured as before. Other similar recipes were formulated with varying fluorinated monomer content so that its influence on the resulting water contact angles (and hence the surface free energies) of the coatings could be obtained.

Coating Formulations with UV Absorber

A final modification to the coating properties involved incorporating an UV absorbing species into the coating formulations to improve the UV resistance of

the coating. Such a coating could also serve to protect a UV-sensitive substrate; however, this was not a concern for the metals. Again it was preferred to covalently bond the UV absorbing species directly to the hybrid network in order to prevent diffusion and loss of the species with time. The UV absorber chosen for this purpose was Norbloc 7966, the structure of which is shown in the reaction scheme outlined in Figure 7. Although (at the time) an alkoxysilane functional UV absorbing species could not be readily found, the Norbloc material has a reactive vinyl group (methacrylate) that was exploited. Alkoxysilanes containing vinyl groups can be readily obtained, and such a molecule can be used as a link between the sol–gel network and the UV absorber. Specifically, trimethoxysilylpropyl methacrylate was used as the linking molecule, the structure of which is also shown in the reaction scheme of Figure 7. This material has a trimethoxysilane group that can participate in the sol–gel reaction, and also a vinyl group that can be polymerized along with the vinyl groups of the Norbloc 7966 material (with added free-radical initiator, benzoyl peroxide). A typical coating formulation [f-DETA(45) TMOS(50) MASi(4) UV(1)] was made by combining 2.00 g IPA, 0.06 g Norbloc 7966, 0.24 g trimethoxysilylpropyl methacrylate (MASi), 3.00 g TMOS, and 3.86 g f-DETA solution and allowing this mixture to stir at ambient conditions until a homogeneous solution results (the Norbloc takes ≈5 to 10 min to dissolve completely). Once a homogeneous solution was formed, 1.00 g 0.3

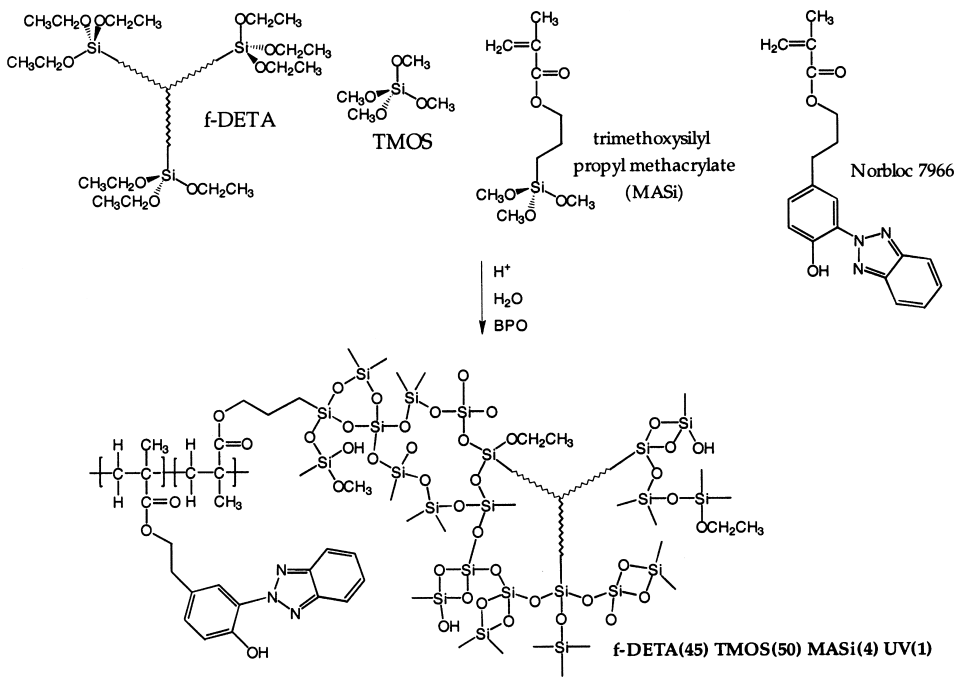

Figure 7. The sol–gel and free radical reactions of f-DETA, TMOS, MASi, and Norbloc 7966, forming a coating designated as f-DETA(45) TMOS(50) MASi(4) UV(1). The resulting structure is meant to reflect an infinite network.

wt% benzoyl peroxide in acetone (initiates methacrylate copolymerization) was added. After allowing ≈1 min for the peroxide to dissolve, 0.34 g 0.5 M HCl was added dropwise while under brisk stirring. This reaction is shown schematically in Figure 7. Such coatings were then applied to the desired substrates and thermally cured as before. It is anticipated that the sol-gel reaction begins immediately after the addition of water and catalyst, whereas the methacrylate polymerization initiates once the coating has been placed in the oven at elevated temperatures.

RESULTS AND DISCUSSION

Aluminum Substrates

A primary goal of this research was to determine the optimum cure temperature and cure time combination for the fundamental f-DETA(100) and f-DETA(50) TMOS(50) coating formulations on aluminum substrates. Previously it had been determined that increasing the cure temperature of such f-DETA-based coatings led to an increase in the abrasion resistance when applied to PC (5). This was thought to be due to the higher extent of reaction attainable at higher temperatures. However, because the glass transition temperature of the PC was ≈145°C, curing above this temperature would cause the substrate to soften and warp from any frozen–in stresses (4). Because this is not a concern for metal substrates, higher temperatures were easily explored. First, a 10-h cure time was held constant while the isothermal cure temperatures of 75, 125, 175, and 225°C were used. It was found that under these conditions both chemistries displayed the best abrasion resistance when cured at 175°C. At 225°C, thermal degradation occurs, manifested as discoloration (golden to brown) of the otherwise transparent coatings. This is believed to be due to the degradation of the urea linkages, which in general are not stable above 200°C for extended periods. At temperatures below 175°C the abrasion resistance is inferior to samples cured at 175°C, due to the lower crosslink density (extent of reaction) of the hybrid network generated at the lower temperatures. Figure 8 shows the influence of cure temperature on the abrasion resistance of f-DETA(50) TMOS(50) coatings on aluminum. Note that the annular wear tracks are most evident on the samples cured at 75 and 225°C, and least visible on the 175°C sample. Cure temperature had a similar effect on f-DETA(100) formulations on aluminum.

It was shown in a previous study (5) that longer curing times led to better abrasion resistance. As previously mentioned, however, the cure temperature for this earlier work was held below 145°C. In the present work, while the cure temperature was held constant at 175°C, cure times of 1, 5, 10, 15, 20, 40, 60, 120, 180, and 600 min were explored. Transferring a coated panel from room temperature directly into a 175°C oven led to bubbling of the coating; therefore, the coated samples were placed in a 35°C oven that was then heated at 5°/min to 175°C and held there for the above times. It was found for the f-DETA(100) coating, a minimum of 40 min of cure time was required for optimum abrasion performance. The

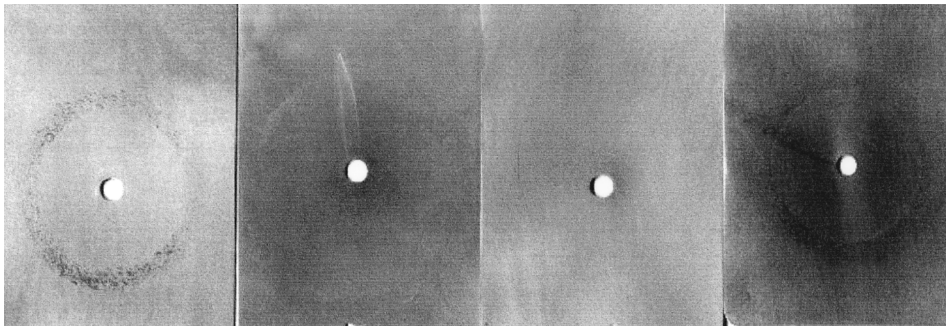

Figure 8. The effect of cure temperature on the abrasion resistance of f-DETA(50) TMOS(50) coatings on aluminum. All samples abraded to 350 cycles. Cure temperatures, from left to right: 75, 125, 175, and 225°C.

f-DETA(50) TMOS(50) system required a shorter cure time of only 20 min for optimum performance. This was determined by the results of the Taber Abraser test as the shortest cure time that displayed the best abrasion resistance (i.e., least obvious wear track by careful inspection). Due to the very slight optical appearance of wear tracks in this aspect of the study, scanned images do not display notable distinctions, and hence, are not presented.

The chemical structure of the network also influences abrasion resistance. For aluminum substrates, both f-DETA(50) TMOS(50) and f-DETA(100) coatings greatly exceeded the performance of the uncoated control sample, as shown in Figure 9. However, it was found that f-DETA(50) TMOS(50) was a distinctly better coating than f-DETA(100) from an abrasion standpoint. This is not difficult to

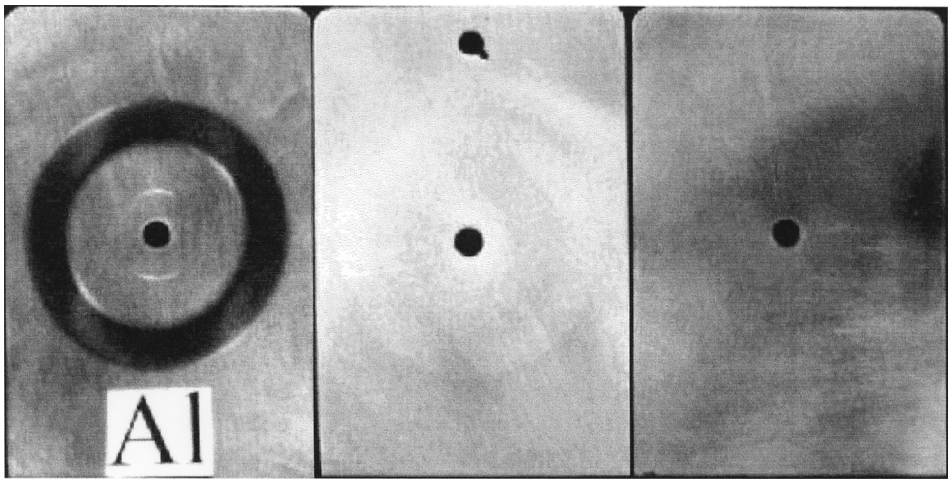

Figure 9. A photograph illustrating coating performance after 350 cycles on aluminum. Uncoated control, left; f-DETA(100), center; f-DETA(50) TMOS(50), right.

perceive from the molecular structure of the cured network; the addition of TMOS to the reaction results in more —Si—O—Si— linkages in the final network (which is much like amorphous silicon dioxide), thereby producing a material with more inorganic content and higher crosslink density. This is expected to produce a harder, more abrasion resistant material. The abrasive wear rate for a large number of pure metals is inversely proportional to their indentation hardness (10,11). Hence, it is a commonly held conception that harder materials are more abrasion resistant. Increasing the relative amount of TMOS in f-DETA-based coatings improved the abrasion resistance accordingly, as wear tracks became less visible with increasing TMOS content. However, for the case of hybrid sol–gel coatings, no clear link exists between the coating hardness and abrasion resistance (6). Other important factors in the wear process that have not been considered include surface roughness, the friction coefficient, and fracture toughness of the coating.

Previous reports (2,3,5) have shown that a tearing mechanism of abrasive wear occurred during the Taber Abraser test for similar hybrid coatings. For the present study, close inspection of an abraded f-DETA(50) TMOS(50) coating on aluminum revealed a similar mechanism of wear (Fig. 10). The criss–cross shape of the wear track was a result of the opposing spin of the two Taber Abraser wheels. Notice that most of the coating surface remained undamaged, and the scratches were for the most part, few in number.

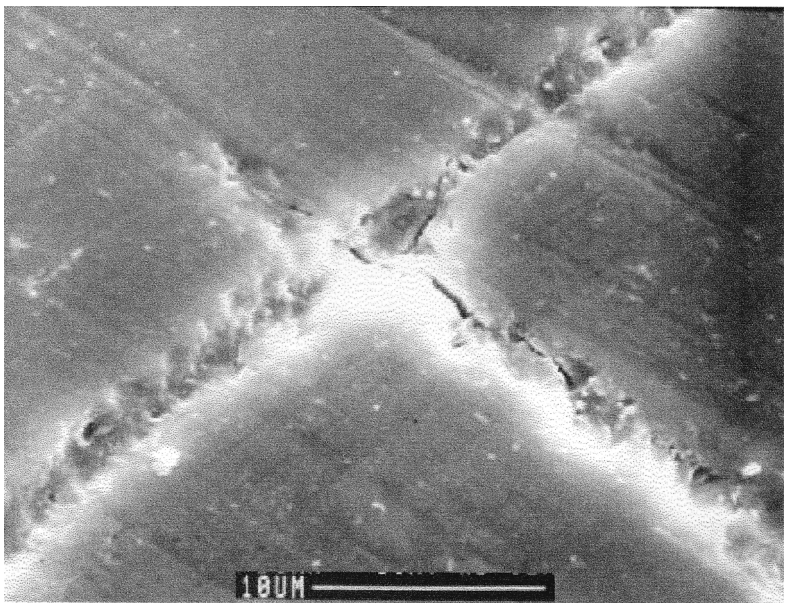

Figure 10. SEM images of part of a wear track in a f-DETA(50) TMOS(50) coating on aluminum after 350 cycles. The images are not of the same area of the coating. 10-μm marker.

Simple salt water immersion tests served as an index of corrosion resistance for these coated systems. A solution of 3.5 wt% NaCl (this is the approximate concentration of dissolved salts in ocean water) in deionized water served as the corroding medium. Samples were either half or completely submersed in the salt water for anywhere from 1 to 7 days. Evaluation of performance was accomplished by the physical appearance after the exposure. Both coating chemistries on aluminum display improved corrosion resistance in the salt water immersion compared with uncoated control samples. After 24-h exposure, the control exhibited pitting corrosion visible to the naked eye. Analogous examination of the coated samples confirmed that no damage was apparent at this level. No distinction could be made between the corrosion resistance of either coating formulation by these experiments.

The effect of adding a fluorinated monomer to the coating formulations was monitored through the measurement of the water contact angle. There was a nearly linear increase in the water contact angle with increasing fluorinated monomer content, as shown in Figure 11. Because fluorinated species are typically expensive, an alternative route was devised to maximize its influence on surface properties. A normal, fluorine-free f-DETA(50) TMOS(50) coating was applied by the spin-coating process to a substrate, and while still spinning, a small amount of the fluorinated monomer (≈5 wt% of the coating formulation) was applied by pipette to the top. This confined the fluorinated material primarily to the surface, hence maximizing its influence there. Note that by coating the fluorinated monomer on top of a normal f-DETA(50) TMOS(50) coating, a high contact angle was observed (90 ± 4° in Fig. 11). Again, this required only ≈5 wt% of the fluorinated monomer. A coating which also contained 5 wt% of the fluorinated monomer, however, distributed throughout the entire coating layer, had a contact angle of only 68 ± 2°. Hence, applying the fluorinated material only to the surface greatly enhanced the water contact angle. It was found that this secondary fluori-

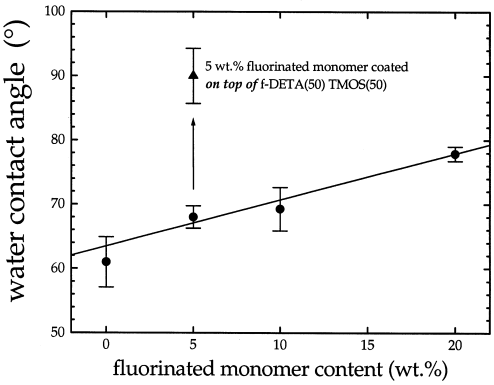

Figure 11. The influence of fluorinated monomer content on the water contact angle of resultant coatings.

Table 1. Results of Direct Pull off Tests for a Few Coating Systems

Substrate	Coating Formulation	Bond Strength (MPa)
Aluminum	f-DETA(50) TMOS(50)	> 20.3
Steel	f-DETA(50) TMOS(50)	> 20.9
Polished aluminum	f-DETA(50) TMOS(50)	> 5.7

nated layer could be applied to the f-DETA(50) TMOS(50) formulation before (recall having 90 ± 4°) *or* after (88 ± 2°) the thermal curing step (of the base f-DETA(50) TMOS(50) layer) with the essentially the same resulting water contact angle. However, the fluorinated layer itself must be thermally cured to generate a durable surface-free energy, so if a previously cured f-DETA(50) TMOS(50) coating is to have a fluorinated layer added to it, the entire sample must be thermally cured a second time after application of the fluorinated species. Such surface-fluorinated coatings were rigorously washed with soap and water, followed by isopropanol, and the contact angle remained essentially the same, ≈87 ± 2°. Table 2 contains the contact angle data for all coating systems containing 5 wt% fluorinated monomer of these different preparation procedures, and as can be seen, all values for the samples that had the fluorinated layer applied on top of the f-DETA(50) TMOS(50) coating were nearly the same. It should be noted that the thin fluorinated layer could be *abraded* away from the surface, leaving a much higher surface-free energy (lower water contact angle) associated with the f-DETA(50) TMOS(50) coating.

Direct pull off tests have failed to provide quantitative coating–substrate adhesion strengths for the coated metals. For every such experiment conducted, failure never occurred at the coating–substrate interface but rather at some other location in the apparatus (usually between the coating and the epoxy adhesive). For this reason it was concluded that the coating–substrate adhesion was quite sig-

Table 2. Water Contact Angles for Coatings Prepared by Various Procedures Containing 5 wt% of the Fluorinated Monomer

Fluorination procedure	Contact angle (°)
fluorinated monomer distributed throughout coating layer	68 ± 2
fluorinated monomer coated *on top* of f-DETA(50) TMOS(50)	90 ± 4
as above, washed vigorously	87 ± 2
fluorinated monomer coated on top of *previously cured* f-DETA(50) TMOS(50), then *cured again*	88 ± 2

nificant, although not rigorously quantified. Therefore, the adhesive strengths thus measured, shown in Table 1, are all listed with a "greater than" symbol due to the lack of failure at the coating–substrate interface. Other adhesives were chosen for use in the direct pull off apparatus in addition to epoxy, e.g., cyanoacrylate, and acrylic, both with the same results as the epoxy. The good adhesion observed for these coating–substrate systems could be partly due to direct covalent bonding between the coating and aluminum surface (12). Surface hydroxyls on the aluminum (which are generally present on many metals) (13) could react with alkoxysilane groups of the coating formulation, thereby generating covalent links (the chemistry is shown schematically in Fig. 12). This is particularly important in explaining the good adhesion between the coatings and the highly polished aluminum substrates (to be addressed in a later section), where mechanical interlocking as a mode of adhesion was not likely to occur. Good adhesion between the ceramer coatings and the aluminum substrates was not a surprising result because silanes are used as coupling agents for bonding various adhesives to metal substrates such as steel, titanium, and aluminum (14,15).

Plain Steel Substrates

For the plain steel substrates the abrasion behavior of the f-DETA(50) TMOS(50) coating was unexpectedly poor (16). During the abrasion test, rather large pieces (~1 mm^2) of this coating detached. This result is unexpected because this same coating displayed excellent performance on aluminum. f-DETA(100) displayed much better performance than did f-DETA(50) TMOS(50) on steel in the abrasion tests. The difference can be seen in Figure 13. The sample with the f-DETA(100) coating showed a relatively uniform wear track (although it was quite pronounced), whereas the sample with the f-DETA(50) TMOS(50) coating was nonuniform in its wear process. The coating on this sample displayed large areas, where complete breakthrough to the steel surface was achieved. Three SEM

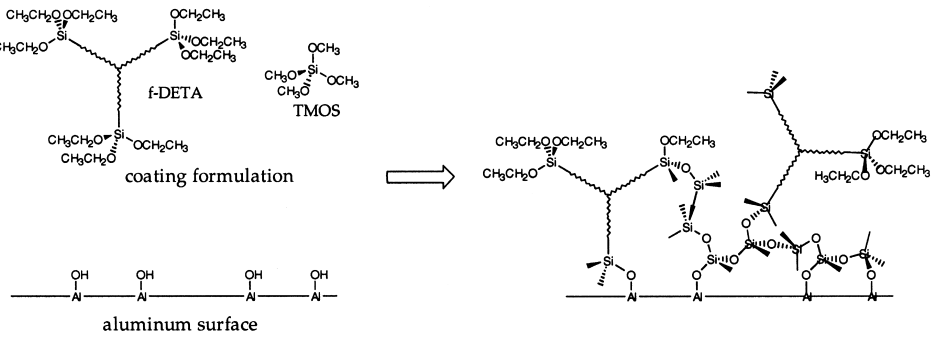

Figure 12. Possible structure at the f-DETA(50) TMOS(50) coating–aluminum substrate interface. Similar structures would exist for other coating formulations and metal substrates as well.

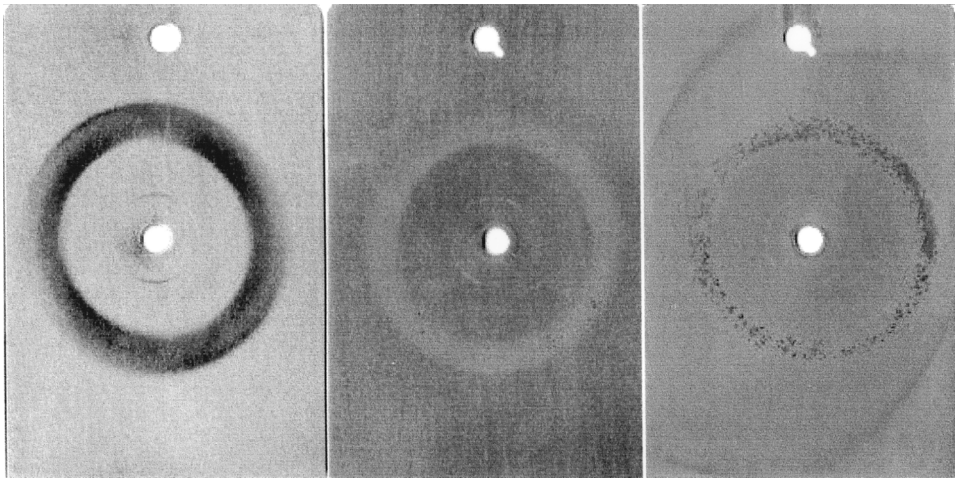

Figure 13. Coating performance after 350 cycles on steel. Uncoated control, left; f-DETA(100), center; f-DETA(50) TMOS(50), right.

images of the same area of an abraded sample, of various magnifications, are shown in Figure 14. The very bright patches are the bare steel surface, where the coating has fractured and detached. Some areas of the surface had a similar criss–cross pattern generated by the tearing mechanism of abrasive wear (as was observed for this coating on aluminum), but the majority of wear in this sample was brittle fracture wear, surface fatigue wear, or perhaps corrosive wear (17,18).

Because a silane may potentially form similar covalent bonds to the steel surface (19) as with the aluminum substrates, some other controlling factor must have been present that led to the poor abrasion performance of the f-DETA(50) TMOS(50) coatings. Recall that both the aluminum and steel substrates were sanded so that mechanical interlocking between the coatings and substrates could take place on both. Also, for both substrates the coating was applied while the viscosity of the mixture was low and, therefore, wetting and spreading was satisfactory. However, because aqueous HCl was present in the coating formulations as a catalyst for the sol–gel reaction, it is possible that this acid may have attacked the steel surface, leading to rapid corrosion. Subsequent curing of the coating would have left a weak boundary layer (corroded, passive oxide layer). It would be expected that rather large pieces of the brittle, corroded layer would detach during the abrasion test, which was observed. This is consistent with the mechanism of corrosive wear (17). The possibility of corrosion as the important factor was supported by the fact that almost twice as much acid was present in the f-DETA(50) TMOS(50) formulation (poor performance) than in the f-DETA(100) formulation (good performance). Corrosion was not evident on a large scale, because no rust was visible. However, the direct pull off test did not show a low value of the f-DETA(50) TMOS(50) coating–steel substrate adhesive strength (Tab. 1). Again the coatings could not be pulled directly off with this test.

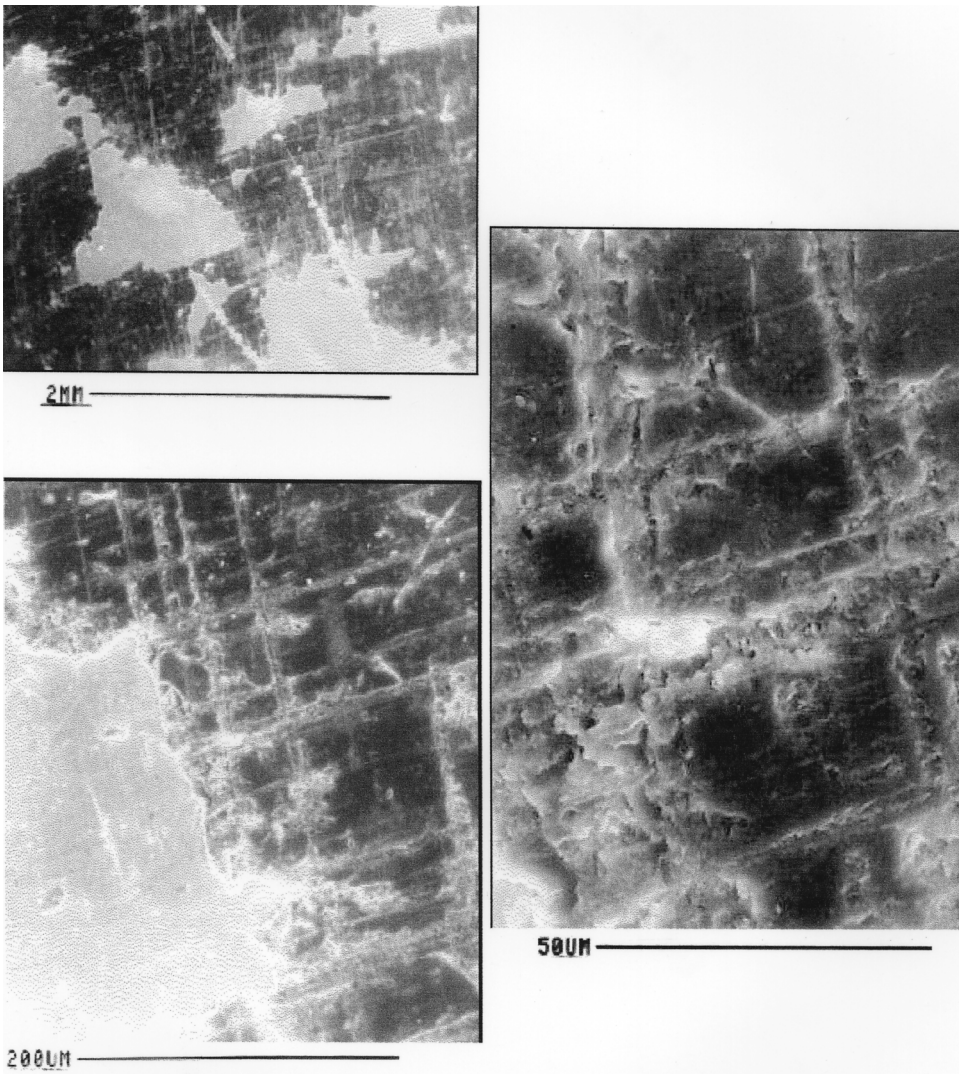

Figure 14. SEM images of an abraded f-DETA(50) TMOS(50) coating on steel after 350 cycles. 2-mm, 200-μm, and 50-μm markers.

Salt water exposure of uncoated steel samples led to pronounced corrosion after 24 h. This was manifested as massive discoloration of the surface of the steel. The f-DETA(100)-coated samples showed no obvious damage after this experiment. An uncoated and f-DETA(100)-coated sample are shown in Figure 15 after a half immersion in salt water for 1 day. The uncoated sample showed massive corrosion (the lower half was exposed to salt water. The corrosion on the upper half occurred later, over time, due to exposure to ambient lab conditions). The f-DETA(100)-coated sample showed no signs of corrosion from the salt water exposure. The "rusty" line seen on this coated sample resulted from corrosion of the

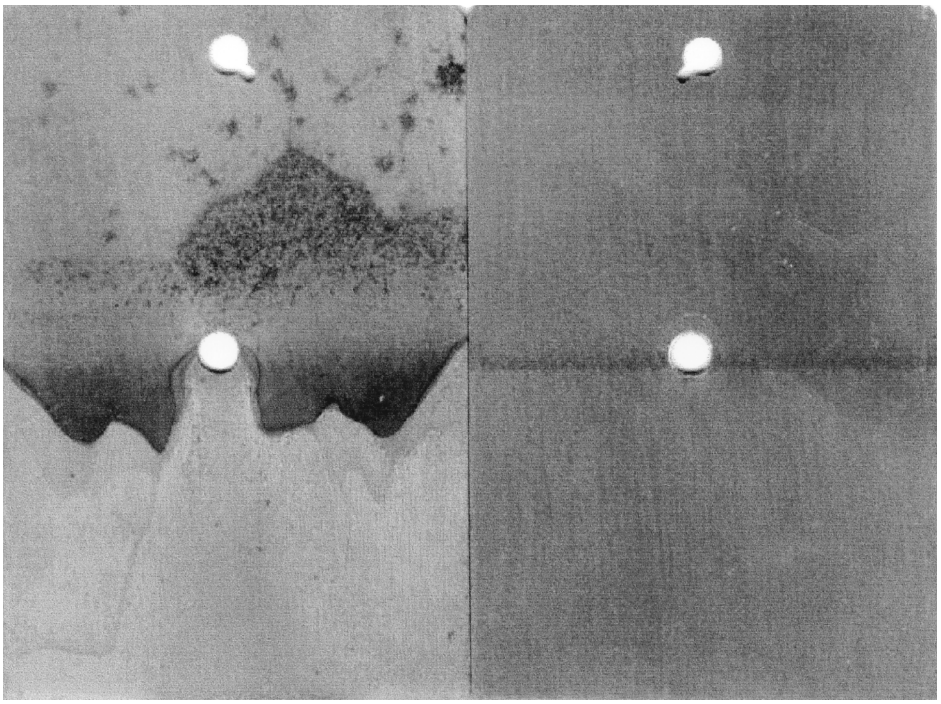

Figure 15. Comparison of the corrosion resistance of uncoated (left) and f-DETA(100) coated (right) steel. Samples were half immersed in salt water.

opposite, uncoated side of the sample. Rust particles detached from the corroded side, floated on the surface of the salt water, and were deposited on the coating at the location of the waterline.

Conversion Coated Steel Substrates

Coatings on the two conversion coated steels behaved similarly to each other. Both f-DETA(100) and f-DETA(50) TMOS(50) coatings were poorly adhered to these substrates after curing. The reason for this is suggested to be due to: 1) a lack of preferred chemical groups at the surface of the substrate, and 2) a lack of sufficient surface roughness. As previously mentioned, these substrates were not sanded due to the thin conversion coatings, and these very smooth surfaces inhibited mechanical interlocking or "keying" as a mechanism of adhesion. Hence, the conversion coated steels provided no advantage over plain steel for our purposes. f-DETA(50) TMOS(50) coatings performed similarly on both the zinc and iron phosphated steels.

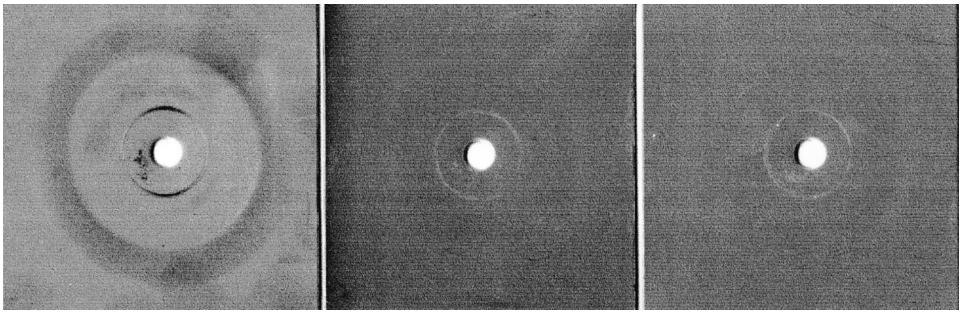

Figure 16. Coating performance on stainless steel substrates after the Taber Abraser test. Uncoated control after 10 cycles, left; f-DETA(50) TMOS(50) coated after 100 cycles, center; f-DETA(50) TMOS(50) coated after 200 cycles, right.

Stainless Steel Substrates

Stainless steel was very well protected from abrasion by f-DETA(50) TMOS(50) coatings, in contrast to the plain and conversion coated steels. Wear track visibility was essentially negligible up to at least *200 cycles* for these coatings, while a clear wear track was apparent after only *10 cycles* for the uncoated substrate (Fig. 16).

Copper Substrates

Copper is a relatively soft metal, although its density is higher than steel (compare 8.9 g/cm^3 with 7.8 g/cm^3) (20). Despite the high density of this metal, ceramer coatings provided abrasion resistance far superior to the bare metal. Figure 17 shows the performance of f-DETA(50) TMOS(50) coatings on copper substrates, compared with an uncoated control. In the uncoated sample, a clear

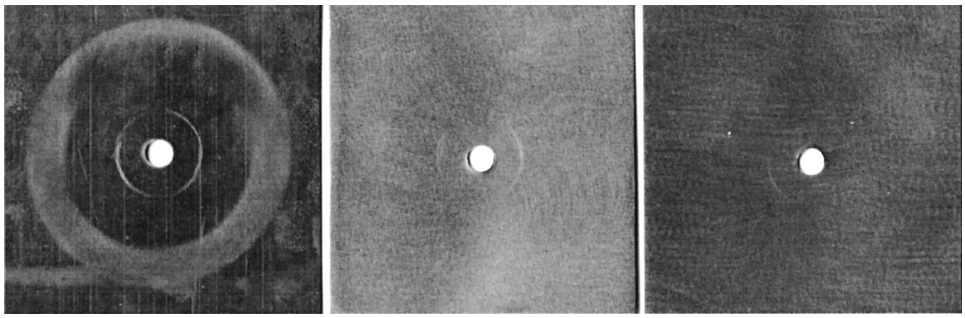

Figure 17. Coating performance on copper substrates after the Taber Abraser test. Uncoated control after 10 cycles, left; f-DETA(50) TMOS(50) coated after 250 cycles, center; f-DETA(50) TMOS(50) coated after 500 cycles, right.

wear track could be seen after only 10 cycles on the Taber Abraser. The two coated samples displayed little evidence of a wear track after 350 and 500 cycles. It is also worthy to note that the coatings on the copper substrates had a pleasing, cosmetic appearance.

Brass Substrates

Figure 18 shows the performance of the f-DETA(50) TMOS(50)-abrasion resistant coating on brass. Again, the uncoated control showed distinct wear after only 10 cycles, whereas the two coated samples exhibited little visible wear after 100 and 200 cycles, respectively.

Polished Aluminum Substrates

The polished aluminum substrates have applications in decorative molding for lighting fixtures, among other areas. This highly polished material is easily abraded; it can even be scratched by lightly rubbing with a Kimwipe®.

Figure 19 shows two coated, polished aluminum substrates [f-DETA(50) TMOS(50) and f-DETA(45) TMOS(50) MASi(4) UV(1)] and an uncoated control after abrasion testing. The control showed massive wear after only two cycles, but the coated substrates showed little wear after 50 cycles.

One of the coatings in this figure [f-DETA(45) TMOS(50) MASi(4) UV(1)] had the UV absorber incorporated. This may prolong the durability of the coating itself, or perhaps can protect a UV-sensitive substrate (such as bisphenol-A polycarbonate). The abrasion resistance of the UV-containing coating was similar to the f-DETA(50) TMOS(50) coating on this polished aluminum substrate.

With these substrates the possibility of stacking coated samples on top of one another before thermally curing the applied coatings has been explored. This

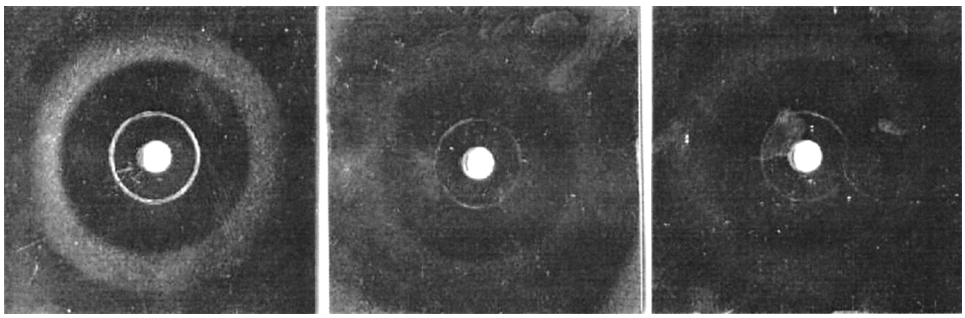

Figure 18. Coating performance on brass substrates after the Taber Abraser test. Uncoated control after 10 cycles, left; f-DETA50-TMOS50 coated after 100 cycles center; f- DETA50-TMOS50 coated after 200 cycles, right.

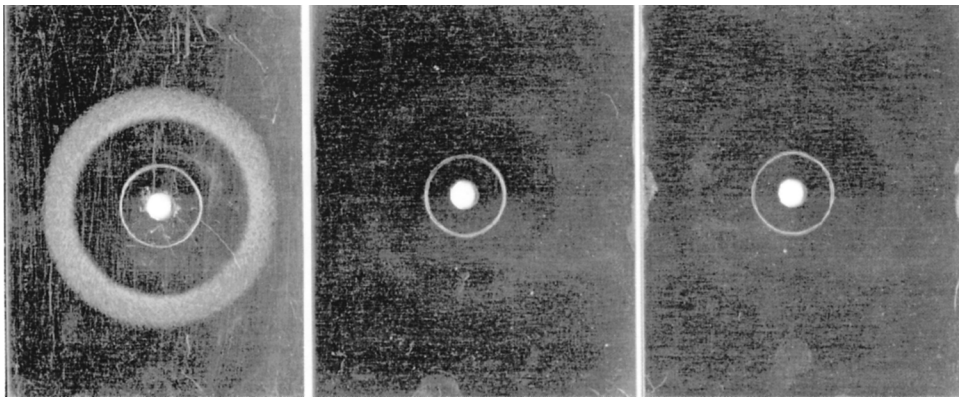

Figure 19. Abrasion test results for polished aluminum substrates. Uncoated control after **two cycles**, left; f-DETA(50) TMOS(50) coated after 50 cycles, center; and a f-DETA(45) TMOS(50) MASi(4) UV(1) coating after 50 cycles, right.

was based on the fact that often coils of aluminum sheeting are generally soon rolled up after coating. To simulate such a situation, two small pieces of sheet were used. They were curved by bending over a cylinder of 18 cm diameter. After applying the coating to the bent sheets and allowing the coatings to reach a nontacky state, the two samples were pressed together with a weight while thermally cured at 175°C. The samples did not stick together during the curing process as long as the coatings were not tacky before stacking the layers. This result provides two potential routes for applying these abrasion resistant coatings to a metal sheet on an industrial scale; while the sheet is unrolled from the spool, it can either have the coating applied, cured, and be rewound, or have the coating applied, dried to a nontack state, be rewound, and later the whole roll could be placed in an oven for curing.

Although the coated samples were bent as described above, the coatings remained adhered on these polished aluminum substrates. In fact, when a sample containing a cured f-DETA(50) TMOS(50) coating was folded over (180° bend) and bent back (0°), the coating still remained adhered.

CONCLUSION

The performance of alkoxysilane functionalized diethylenetriamine-based ceramer coatings applied to various metal substrates was probed. In general, increasing the TMOS content led to a more abrasion-resistant coating. An optimum cure temperature of 175°C was determined. This temperature was higher than conventional cure temperatures used for such coatings on bisphenol–A polycarbonate, due to the limitations of the glass transition temperature of this substrate. At a cure temperature of 175°C, an optimum cure time of 40 min was found for f-DETA(100) and 20 min for f-DETA(50) TMOS(50) coatings. Adhesion

between the coatings and aluminum substrates was found to be excellent, although not quantified. Direct pull off tests did not remove the coating from the substrates, but rather the failure occurred at the epoxy/coating interface in these tests. It was conjectured that the coatings form direct covalent bonds to surface hydroxyls on the metal substrates, thereby contributing to the excellent observed adhesion. f-DETA(50) TMOS(50) coatings on plain steel and the two conversion coated steels performed poorly in the abrasion tests. This was proposed to be due to corrosion of the steel by the acid catalyst in the case of plain steel and undesirable surface chemistry in the case of the phosphated panels. f-DETA(50) TMOS(50) coatings protected stainless steel, copper, and brass extremely well from abrasion. A fluorinated alkoxysilane monomer was incorporated into the coating formulations, which led to a systematic increase in the water contact angle of the resulting coatings. A UV absorber was also incorporated into the ceramer coatings, through a covalent bonding process, in an attempt to lengthen the lifetime of the coatings in a UV environment.

ACKNOWLEDGMENTS

We thank the Center for Adhesive and Sealant Science at Virginia Tech, as well as the Adhesive and Sealant Council Education Foundation for their financial assistance. We would like to thank Professor James Wightman for use of his contact angle goniometer.

REFERENCES

1. Wilkes, G.L.; Orler, B.; Huang, H. Am. Chem. Soc., Div. Polym. Chem. (Polymer Preprtints). **1985**, *26(2),* 300.
2. Tamami, B.; Betrabet, C.; Wilkes, G.L. Polym. Bull. **1993**, *30*, 39.
3. Tamami, B.; Betrabet, C.; Wilkes, G.L. Polym. Bull. **1993**, *30*, 393.
4. Wang, B.; Wilkes, G.L.J. Macromol. Sci.,—Pure & Appl. Chem. **1994**, *A31(2),* 248.
5. Wen, J.; Wilkes, G. L.J. Inorg. Organomet. Polym. **1995**, *5(4),* 343.
6. Wen, J.; Vasudevan, V. J.; Wilkes, G.L.J. *Sol–Gel Sci. Tech*. **1995**, *5*, 115.
7. Wen, J.; Jordens, K.; Wilkes, G.L. In *Better Ceramics Through Chemistry VII: Organic/Inorganic Hybrid Materials;* Coltrain, B.K.; Sanchez, C.; Schaefer, D.W.; Wilkes, G.L., Eds.; Mater. Res. Soc. Symp. Proc. **1996**, *435*, 207.
8. Croll, S.G. Adhesion and Internal Strain in Polymeric Coatings. In *Adhesion Aspects in Polymeric Coatings*; Mittal, K.L., Ed.; Plenum Press: NY, 1983.
9. Shaw, D.J. *Introduction to Colloid and Surface Chemistry*, 3rd Ed.; Butterworths: London, 1980.
10. Kruschov, M. M. Proc. Conf. Lubrication Wear. **1957**, 655.
11. Rabinowicz, E.; Dunn, L.A.; Russell, P.G. Wear **1961**, *4,* 345.
12. Kinloch, A.J.; Dukes, W.A.; Gledhill, R.A. Durability of Adhesive Joints. In *Polymer Science and Technology*, Vol. 9B; 597. *Adhesion Science and Technology*; Lee, L.–H. Ed.; Plenum Press: New York, 1975.

13. Minford, J.D. Adhesives. *In Durablility of Structural Adhesives*; Kinloch, A. J., Ed.; Applied Science Publishers: New York, 1983; 135. See particularly Figure 3 of p. 150.
14. Aker, S.C. The Function of Adhesive Primers in Adhesive Bonding of Aircraft Structures. In *Appl. Polym. Symp*., *19*, Processing for Adhesives Bonded Structures; Bodnar, M.J., Ed.; John Wiley & Sons: New York, 1972.
15. Kinloch, A.J. *Adhesion and Adhesives: Science and Technology*; Chapman and Hall: NY, 1987.
16. Jordens, K.; Wilkes, G. L. *PMSE Preprints* **1995***, 73*, 290.
17. Rabinowicz, E. *Friction and Wear of Materials*; John Wiley & Sons: New York, 1965.
18. *Principles of Tribology*; Holling, J., Ed.; The Macmillan Press Ltd.: London, 1975, 1978.
19. Gettings, M.; Kinloch, A. J. J. Mater. Sci. **1977**, *12*, 2511.
20. CRC Handbook of Chemistry and Physics, 68th Ed.; Weast, R.C., Ed.; CRC Press, Inc.: Baton Roca, FL, 1987; B-88.

Received December 11, 1999
Revision received September 15, 2000